as the summation of the result in the case of $r_2 \geq r_1$ and that in the case of $r_1 > r_2$.

References and Notes

(1) Presented in part at the 28th Annual Meeting of the Society of Polymer Science, Japan, Tokyo, May 1979. (b) Yamagata University. (c) Nara Women's University.
(2) Toth, W. J.; Tobolsky, A. V. *J. Polym. Sci., Polym. Lett. Ed.* **1970**, *8*, 531.
(3) Stamatoff, J. B. *Mol. Cryst. Liq. Cryst.* **1972**, *16*, 137.
(4) Iizuka, E. *Biochim. Biophys. Acta* **1969**, *175*, 457.
(5) Iizuka, E. *Biochim. Biophys. Acta* **1971**, *243*, 1.
(6) Iizuka, E.; Keira, T.; Wada, A. *Mol. Cryst. Liq. Cryst.* **1973**, *23*, 13.
(7) Williams, R. *J. Chem. Phys.* **1963**, *39*, 384.
(8) Heilmeier, G. H. *J. Chem. Phys.* **1963**, *44*, 644.
(9) Tsuboi, M. *J. Polym. Sci.* **1962**, *59*, 139.
(10) O'Konski, C. T.; Yoshioka, K.; Orttung, W. H. *J. Phys. Chem.* **1959**, *63*, 1558.
(11) Watanabe, H.; Yoshioka, K.; Wada, A. *Biopolymers* **1964**, *2*, 91.
(12) Sobajima, S. *J. Phys. Soc. Jpn.* **1967**, *23*, 1070.
(13) Orwell, R. D.; Vold, R. L. *J. Am. Chem. Soc.* **1971**, *93*, 5335.
(14) Iizuka, E.; Go, Y. *J. Phys. Soc. Jpn.* **1971**, *31*, 1205.
(15) Samulski, E. T.; Tobolsky, A. V. *Macromolecules* **1968**, *1*, 555.
(16) Wilkes, G. L. *Mol. Cryst. Liq. Cryst.* **1972**, *18*, 165.
(17) Robinson, C. *Trans. Faraday Soc.* **1956**, *52*, 571.
(18) Robinson, C.; Ward, J. C.; Beevers, R. B. *Discuss. Faraday Soc.* **1958**, *25*, 29.
(19) Robinson, C. *Tetrahedron* **1961**, *13*, 219.
(20) Rhodes, M. B.; Stein, R. S. *J. Polym. Sci., Part A-2* **1969**, *7*, 1539.
(21) Stein, R. S.; Rhodes, M. B. *J. Appl. Phys.* **1960**, *31*, 1873.
(22) Stein, R. S.; Wilson, P. R. *J. Appl. Phys.* **1962**, *33*, 1914.
(23) Clough, S.; van Aartsen, J. J.; Stein, R. S. *J. Appl. Phys.* **1965**, *36*, 3072.
(24) Stein, R. S.; Erhardt, P. F.; Clough, S. B.; Adams, G. *J. Appl. Phys.* **1966**, *37*, 3980.
(25) Rhodes, M. B.; Porter, R. S.; Chu, W.; Stein, R. S. In "Liquid Crystals"; Gordon and Breach Science Publishers: New York, 1969; Vol. II.
(26) Picot, C.; Stein, R. S. *J. Polym. Sci., Part A-2* **1970**, *8*, 1491.
(27) Stein, R. S.; Chu, W. *J. Polym. Sci., Part A-2* **1970**, *8*, 1137.
(28) Hashimoto, T.; Stein, R. S. *J. Polym. Sci., Part A-2* **1971**, *9*, 1747.
(29) Stein, R. S.; Hashimoto, T. *J. Polym. Sci., Part A-2* **1971**, *9*, 517.
(30) Hashimoto, T.; Murakami, Y.; Hayashi, N.; Kawai, H. *Polym. J.* **1974**, *6*, 132.
(31) Hayashi, N.; Murakami, Y.; Moritani, M.; Hashimoto, T.; Kawai, H. *Polym. J.* **1973**, *4*, 560.

Neutron Scattering Studies on the Conformation of Atactic Polystyrene Chains in a Bulk-Crystallized Isotactic Polystyrene

Jean-Michel Guenet* and Claude Picot

Centre de Recherches sur les Macromolécules (CNRS), 67083 Strasbourg Cedex, France.

Received February 12, 1980

ABSTRACT: The conformation of atactic polystyrene in a semicrystalline isotactic polystyrene matrix has been determined through the use of small-angle neutron scattering. Keeping the concentration of the deuterated atactic species constant ($C_D \sim 1\%$), we have systematically varied the degree of crystallinity of the sample by two methods: (1) by annealing the samples for different times at $T_c = 180$ °C (system A); (2) by introducing increasing amounts of hydrogenated atactic polystyrene and keeping the annealing time constant (system B). In system A, the results show that chains are excluded from the crystallizing regions for low crystallinities. For the highest crystallinities, the experimental results suggest that the chains are trapped and extended within the fibrils and the short-range structure is far from the Gaussian. In system B, the chains remain elongated but the subunits recover their Gaussian statistic. Viscoelastic properties of melt polymers are used to provide explanations for these results, which are also discussed in regard to other works performed on similar samples.

Introduction

Many papers have been devoted to the rejection of noncrystallizable materials during the crystallization process of stereoregular polymers.[1-6] For example, the stereoirregular structure of atactic polystyrene (APS) not only hinders its crystallization but also makes it unlikely that it can be incorporated, to any significant extent, within the crystals of the corresponding stereoregular polymer. Some years ago, Keith and Padden[1] studied by optical microscopy the spherulitic structure of the same system. By modifying the content of impurities (i.e., APS content) in a blend with isotactic polystyrene (IPS), they showed that the interfibrillar melt is composed of mainly atactic material which has been rejected at the tips of the growing fibers.

These interpretations are in agreement with those given by Yeh and Lambert[2] based on kinetic studies. These authors concluded, by measuring the variations in spherulitic growth rate as a function of molecular weight of the atactic species, that above $M_w = 5 \times 10^4$ significant amounts of noncrystallizable rejected chains are trapped within the growing spherulites and that they probably reside in the interfibrillar domain as opposed to the interlamellar regions.

More recently, Stein and co-workers[3] examined the lamellar structure in these blends by small-angle X-ray scattering (SAXS). Upon addition of the atactic "impurity", they found an invariance of the interlamellar distance as well as an invariance in lamellar stacking parameters as ascertained by application of the Hosemann paracrystalline model.[7] In view of these results, they concluded that the findings of Keith and Padden and Yeh and Lambert are qualitatively correct. That is, since rejected material is not incorporated into the interlamellar regions, it must be included in the interfibrillar melt.

The purpose of this paper is to extend these previous works to the determination of the chain conformation of the rejected species, which may be accomplished through the use of small-angle neutron scattering (SANS). With this technique, a small amount of the atactic chains may be preferentially deuterium labeled, which allows their isolated behavior to be determined directly in the bulk state.[8,9] This paper will examine the effects of both annealing time and addition of hydrogenated atactic species on the conformation of deuterated atactic polystyrene chains in the bulk blend with isotactic polystyrene.

Sample Preparation and Description

Isotactic polystyrene was synthesized at 80 °C in heptane with $Al(C_2H_5)_3$–$TiCl_4$ as catalyst according to the well-known Natta method.[10] After extraction of the atactic material in boiling heptane and in methyl ethyl ketone, the molecular weights deduced from GPC[11] were $M_w = 8.75 \times 10^5$ and $M_n = 1.5 \times 10^5$.

0024-9297/81/2214-0309$01.25/0

Table I
Characteristics and Experimental Results for Samples A[a]

sample	M_{wAPSD}	annealing time	x_c	R_g, Å	$R_{g\Theta}$, Å	$N_{c\ app}$	A_2, cm^3 g^{-2}	p
A-57-0	5.7×10^4	0	0	58	59			$p = 2$
A-57-32		50 min	0.32	438		6	-4.5×10^{-4}	$p = 2$
A-57-45		24 h	0.45					$p_1 = 1.6, p_2 = 3.7$
A-114-0	1.14×10^5	0	0	80	87			
A-114-32		50 min	0.32	536		3	-2.7×10^{-4}	$p = 2$
A-114-45		24 h	0.45					$p_1 = 1.7, p_2 = 3.9$
A-170-0	1.7×10^5	0	0	110	120			$p = 2$
A-170-18		20 min	0.18	210		2		$p = 2$
A-170-24		30 min	0.24	540		2	-1.3×10^{-4}	$p_1 = 1.7, p_2 = 3.9$
A-170-32		50 min	0.32	650		2		$p_1 = 1.5, p_2 = 3.6$
A-170-45		24 h	0.45					$p_1 = 1.7, p_2 = 3.6$

[a] Crystallinities have been determined by density measurements. $R_{g\Theta}$ is the dimension in Θ solvent or atactic bulk.[8] The accuracy of the determination of R_g after crystallization is not of sufficient precision due to segregation. Accordingly, the values given here are only indications and should not be regarded as absolute.

Table II
Characteristics and Experimental Results for Samples B[a]

sample	X_{APS}	M_{wAPSH}	R_g, Å	$N_{c\ app}$	C_{DR}, g cm^{-3}	A_2, cm^3 g^{-2}	p
B-5.5-10	0.1	5.5×10^5			11×10^{-2}		$p_1 = 1.5, p_2 = 2$
B-5.5-15	0.15				7×10^{-2}		$p_1 = 1.4, p_2 = 2$
B-5.5-20	0.20		500	3	5.5×10^{-2}	-1.8×10^{-4}	$p_1 = 1, p_2 = 2$
B-5.5-25	0.25				4.4×10^{-2}		$p_1 = 1, p_2 = 2$
B-1.4-20	0.20	1.4×10^5	420	3	5.5×10^{-2}	-1.8×10^{-4}	$p_1 = 1.54, p_2 = 2$
B-1.4-25	0.25				4.4×10^{-2}		$p_1 = 1.5, p_2 = 2$

[a] Annealing time 70 min at $T_c = 180$ °C. X_{APS} is the weight fraction of the total amount of atactic polystyrene in the sample. Molecular weight of the tagged chains $M_{wAPSD} = 1.7 \times 10^5$.

Tacticity measurements (^{13}C NMR) led to a stereoregularity higher than 95%.[11] Hydrogenated and deuterated atactic polystyrenes (APSH and APSD) were prepared by anionic polymerization.[12]

Blends were prepared by dissolving the weight fractions of each polymer in boiling chlorobenzene at a 1% concentration and coprecipitating the solution into a large excess of methanol by dropwise addition. The dried blends were molded at 250 °C under vacuum, leading to transparent disk-shaped samples of about 1-mm thickness. Crystallizations from the amorphous state were carried out in a mold sealed from the atmosphere.

The experiments have been performed on two different series of samples. In the first series, designated as "sample A", the blends are composed of very small amounts of APSD (1%) in a hydrogenated IPS matrix. The molecular weight of the matrix has been kept constant while those of the tagged chains have been varied between $M_w = 5.7 \times 10^4$ and $M_w = 1.7 \times 10^5$. The crystallinity of these samples has been altered by varying the annealing time for a crystallization temperature $T_c = 180$ °C. In the second series, designated as "samples B", the blends are always composed of very small amounts of APSD (1%) of the same molecular weight ($M_w = 1.7 \times 10^5$) but hy drogenated atactic polystyrene has been added to the IPS matrix. Hydrogenated APSH having two different molecular weights ($M_w = 1.4 \times 10^5$ and $M_w = 5.5 \times 10^5$) have been used separately. For this series of samples the annealing time has been held at $t = 70$ min for $T_c = 180$ °C. The characteristics of all the samples are available in Tables I and II.

Neutron Scattering

A. Theory. For experiments on polymeric systems, two principal properties differentiate SANS from other techniques: the scattering by the sample depends only on the neutron–nucleus interactions, different for H and D atoms; the available wavelength (5–12 Å) leads to values of the scattering vector $q = (4\pi/\lambda) \sin(\theta/2)$ which are inaccessible to light and X-ray scattering and in a range characteristic of current macromolecular distances. Isotopic substitution in conjunction with SANS experiments provides a powerful method of labeling molecules without significantly altering their physicochemical properties.[13]

The coherent intensity scattered by isolated chains within a hydrogenated surrounding is generally written

$$I(q) = KM_wC_D\nu^2P(q) \quad (1)$$

where the constant depends on the camera configuration, C_D is the concentration of the labeled chains in g/cm^3, ν^2 is the contrast factor, and $P(q)$ is the form factor. The form factor $P(q)$ behaves differently depending on the conformation and it is generally examined in two different q domains.

Guinier Range. In this range, for which $qR_g \ll 1$ (R_g being the radius of gyration), $I(q)$ may be written

$$I(q) \sim \nu^2M_wC_D(1 - q^2R_g^2) \sim \nu^2M_wC_D \exp[-q^2R_g^2/3] \quad (2)$$

Analysis of the form factor in this region results in the determination of two important parameters: the radius of gyration, R_g, and from absolute intensity measurements the weight-average molecular weight, M_w.

Intermediate Range ($qR_g \gg 1$ and $ql \ll 1$). In this domain $I(q)$ generally reaches an asymptotic behavior which can be expressed as

$$I(q) \sim 1/q^p \quad (3)$$

where p depends on the conformation. For instance, $p = 1$ corresponds to a rod, $p = {}^5/_3$ to a polymer chain in a good solvent, $p = 2$ to a Gaussian chain, and $p = 4$ to hard spheres or a system having two densities. On the other hand, it must be noted, as has been pointed out for semidilute solutions,[14] that p can take two different values in this range. Then two regimes appear, defining a crossover scattering vector q^* to which corresponds a characteristic length ξ. For distances larger than ξ, one observes the global conformation whereas for distances smaller than ξ, short-range interactions are predominant.

For the problem we are interested here, the possible effect of clustering must be considered. In the Appendix calculations are developed for the scattered intensity of Gaussian chains segregating by rejection into the residual melt.

B. Experiments. SANS measurements were preformed with D11 and D17 cameras available in the Institut Laue-Langevin (Grenoble, France). For each apparatus, the range of scattering vectors was $5 \times 10^{-3} \le q$ (Å^{-1}) $\le 10^{-2}$ for D11 and $10^{-2} \le q$ (Å^{-1}) $\le 8 \times 10^{-1}$ for D17.

In the two cases, a mechanical wavelength selector was used, providing a spectrum characterized by a relative width at half-height $\Delta\lambda/\lambda \sim 10\%$. The experimental setup is describe in ref 15. Calibration has been achieved by using amorphous samples

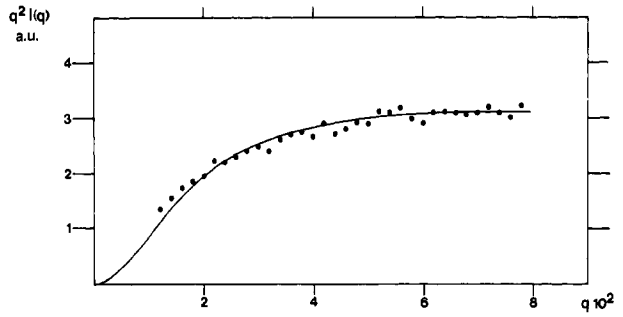

Figure 1. Kratky plot for sample A-170-0. Full line is calculated by using a Gaussian form factor $P_G(q)$ (relation 4) with R_g = 80 Å.

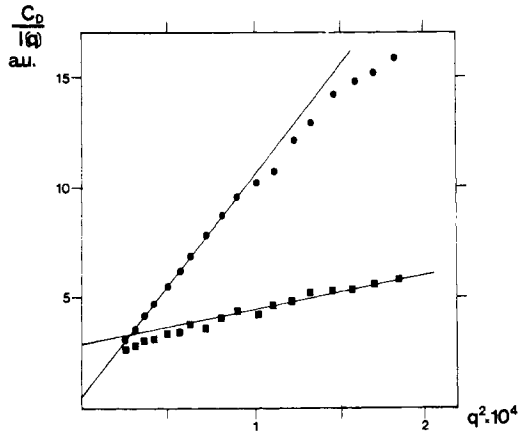

Figure 2. Zimm plot for (●) A-114-32 and (■) A-114-0.

of well-characterized molecular weights.

Results and Discussion

A. Effect of Annealing Time (Samples A). The results presented in this section have been obtained at a fixed concentration of deuterated species ($C_D \sim 1$–1.5%). The results obtained both in the Guinier range and in the intermediate range are listed in Table I.

One notes immediately that dimensions in the amorphous IPS matrix are comparable with those obtained with atactic or Θ-solvent matrices.[8] Under these circumstances, atactic chains are Gaussian. This is also confirmed by the q^{-2} dependence of the scattered intensity in the intermediate range as drawn in Figure 1 according to a Kratky representation. This result is not unexpected despite anomalies recently revealed on inverse systems[16] (IPSD at 1% concentration in APSH matrices).

For the semicrystallized samples, one observes an increase of intensity in the Guinier range (Figure 2) in regard to the above results. This may be explained by considering either a virial effect arising from an attraction between chains or a clustering of N_c chains. Indeed, the intensity may be written two different ways: For labeled chains attracting each other without effective contacts (see Appendix)

$$I(q) = KC_D M_w P_G(q)[1 - 2A_2 C_D M_w P_G(q)] \quad (4)$$

Here A_2 is negative and can be evaluated from experimental results by using amorphous samples to determine the intercept at $C_D = 0$. For an object made of N_c clustered chains (with effective contacts)

$$I(q) = KC_D M_w N_c P_{N_c}(q) \quad (5)$$

$P_{N_c}(q)$ can be evaluated from a model of Gaussian clustered chains as reported in the Appendix. Furthermore, the

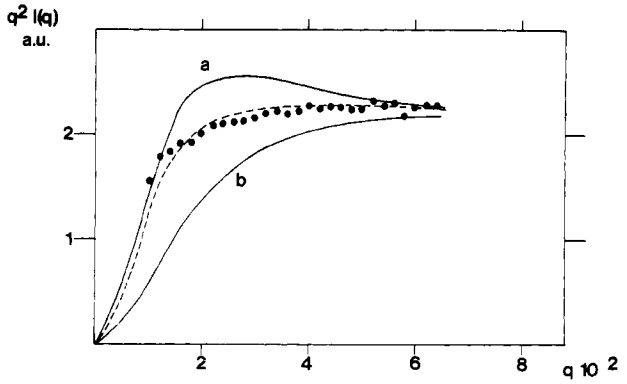

Figure 3. Kratky plot for sample A-114-32. Dotted line is calculated from relation 4 with R_g = 80 Å and A_2 : -2.8×10^{-4}. Full line a is calculated from relation 18 with R_g = 80 Å and N_c = 3. Full line b is calculated from relation 6 (Gaussian form factor).

behavior of intensities in the intermediate range shows that two different conformations may be detected, depending on the degree of crystallinity and on the molecular weight of the atactic labeled chains:

(i) At the initial stage of the crystallization process, the scattering function of the atactic labeled chains exhibits Gaussian exponents (see Table I where $p = 2$). Despite this value of p, the experimental results cannot be correctly fitted with the classical Debye form factor $P_G(q)$ for Gaussian chains (see Figure 3)

$$P_G(q) = \frac{2}{q^4 R_g^4}[\exp(-q^2R_g^2) + q^2R_g^2 - 1] \quad (6)$$

In this case the use of relation 4 allows a better fit of the experimental results (Figure 3). The negative virial coefficient suggests then an attraction between uncrystallizable labeled chains, which arises certainly from their progressive rejection into the residual melt, reducing their mutual average distance that they should have for such a concentration. However, the chain statistic is unperturbed and remains Gaussian. Such a situation occurs only with the atactic chains of smallest molecular weight for $x \leq 0.32$ or of highest molecular weight for $x \leq 0.2$ (as seen in Table I).

(ii) At the final stage of the crystallization process, the labeled chains no longer behave in a Gaussian-like manner and two regimes appear, defining a crossover scattering vector $q^* = 3.3 \times 10^{-2}$, a value found whatever the labeled chains' molecular weight. For $q < q^*$, $I(q)$ behaves like $q^{-1.5}$ to $q^{-1.7}$ and like $q^{-3.6}$ to $q^{-3.9}$ for $q > q^*$ (Figure 4).

Experimental exponents p = 1.5–1.7 are compatible with extended or partially extended particles. Such an assumption seems to be supported by the experiments detailed in the next section.

The extension of the atactic chains can have two origins: (i) the interfibrillar distance is larger than the chain dimension and the shear rate produced between two growing fibers may be sufficiently important to extend the chains; (ii) the interfibrillar distance is smaller than the chain dimension and cannot accommodate the chain in its Gaussian state. Then the effect of the two crystalline barriers leads to a somewhat extended conformation.[17]

As the above exponents have been found whatever the molecular weights of the chains for the highest degree of crystallinity, it seems certain that these two effects take place.

Two explanations may be given concerning the exponents p = 3.6–3.9 defining the short-range conformation:

1. These exponents are compatible with collapsed subunits. As these subunits have very short relaxation

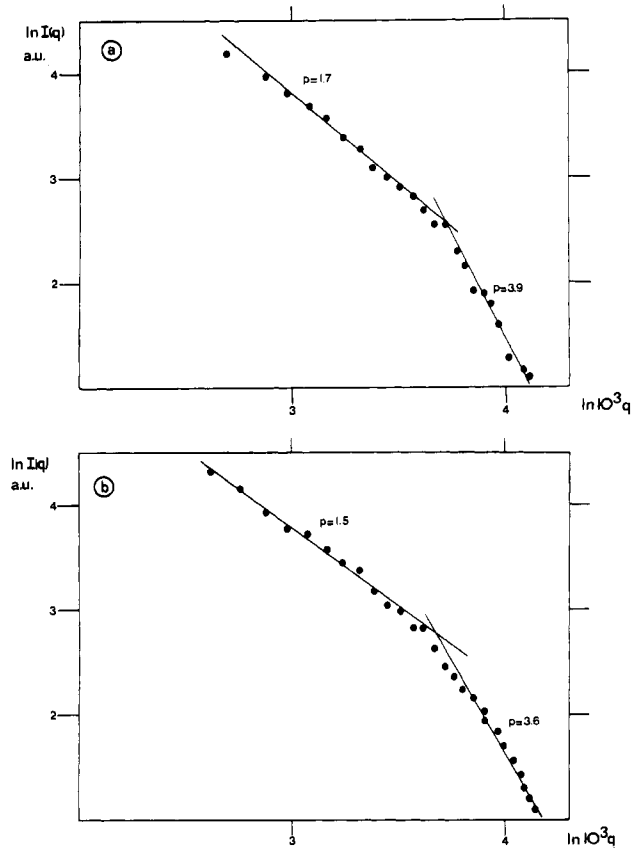

Figure 4. log $I(q)$ vs. log q: (a) sample A-170-24; (b) sample A-170-32.

times, one can guess that they are able to recover their initial Gaussian structure. One explanation of the "collapsing" effect may be given by supposing that the interfibrillar distance is not sufficiently large to allow any accommodation of a Gaussian conformation. Consequently, the subunits would shrink, leading to a "collapsed" structure. One may estimate the approximate size ξ_s of these subunits according to

$$\xi_s = 2/q^* \sim 60 \text{ Å} \tag{7}$$

This distance seems to be too small compared to the interfibrillar distance or even to the interlamellar distance. Therefore this assumption about the subunits structure is not consistent with all the experimental results.

2. Due to segregation, labeled chains form a three-dimensional body within the interfibrillar melt. Then, one should find an exponent close to $p = 4$ in the intermediate range. However, one must keep in mind that amorphous links of isotactic chains are present in these domains so that one is not really dealing with a two-density system. Moreover, at wider angles ($q = 6 \times 10^{-2}$, to which correspond distances of the order of 20 Å), one should retrieve the Gaussian behavior since the scattering function is no longer perturbed by the segregation effect. Since this has not been observed experimentally, this model cannot explain the exponents derived from Figure 4.

From these considerations, we have no satisfactory explanations for these unexpected exponents. It is shown in the next section that this effect vanishes with addition of hydrogenated atactic species.

In summary, whether the chain behavior is Gaussian or not depends both on the molecular weight of the atactic chains and on the overall crystallinity. For the highest degrees of crystallinity, chains were always found to give a somewhat extended conformation. This result may be explained through consideration of the rate of chain mobility in the melt with respect to the rate of the crystalline growth in a matter similar to that used by Keith and Padden.[1] We can compare the distances $\langle \Delta x^2 \rangle^{1/2}$ and y through which have moved, respectively, the atactic chains by Brownian motion and the crystalline growth front for a given length of time t. $\langle \Delta x^2 \rangle^{1/2}$ may be evaluated to a first approximation as

$$\langle \Delta x^2 \rangle^{1/2} = (2Dt)^{1/2}$$

where D is the diffusion coefficient in the molten state. For y we have the relation

$$y = Gt$$

where G is the radical crystalline growth rate.[18] A rough comparison can be made for $t = 1$ s. Calculating D from a relation derived by Bueche[19] and using values of viscosity obtained by Suzuki and Kovacs,[20] one is led to the following results: $M_w = 1.14 \times 10^5$, $\langle \Delta x^2 \rangle^{1/2} \simeq 150$ Å, $y \simeq 50$ Å; $M_w = 1.7 \times 10^5$, $\langle \Delta x^2 \rangle^{1/2} \simeq 50$ Å, $y \simeq 50$ Å.

From these considerations, it seems quite probable that the chains of lowest molecular weight are able to escape temporarily the crystallizing regions while those of higher molecular weight are rapidly overtaken by the growing fibers and extended. Furthermore, the difference of chain mobility should induce the rejection of more chains of low molecular weight as emphasized by Yeh and Lambert[2] into the residual amorphous regions. This assumption is in agreement with the experimental values of either apparent clustering numbers of negative virial coefficients.

B. Addition of Hydrogenated Atactic Species (Samples B). The conformational studies in a bulk-crystallized medium containing increasing amounts of protonated atactic polystyrene (APSH) have been undertaken with a single type of atactic labeled chains ($M_w = 1.7 \times 10^5$) of global concentration in the samples $C_D = 10^{-2}$ g/cm^3.

Before discussing the experimental results listed in Table II, we have to define a "rejection concentration" C_{DR} corresponding to the concentration of the atactic deuterated species with respect to the weight fraction X_{APS} of total atactic polymer in the sample. We then have the relation

$$C_{DR} = C_D/X_{APS} \tag{8}$$

We must keep in mind that, as shown by Keith and Padden, all the atactic species will be assembled together after crystallization.[1-3] This will increase the concentration of labeled chains in the atactic-rich domains and will affect $I(q)$, particularly in the Guinier range. Thus, estimating roughly the overlapping concentration for tagged chains involved in this section

$$C_D^* M_w / 4N_A R_g^3 \simeq 5 \times 10^{-2} \text{ g/cm}^3 \tag{9}$$

we can evaluate to a first approximation the importance of intermolecular interactions and their influence on $I(q)$ after rejection:

For $C_{DR} > C_D^*$, tagged chains will be interpenetrating and $I(q)$ will be even affected in the intermediate range (see Appendix). It must be emphasized here that this effect is possible due to the fact that A_2 is different from 0.

For $C_{DR} \leq C_D^*$, labeled chains are no longer interpenetrating. Then the virial effect is only important in the Guinier range. Intensity in the intermediate range is not affected.

Then the value of C_{DR} is an essential parameter for interpreting and discussing the experimental results. In this section, we essentially examine the asymptotic be-

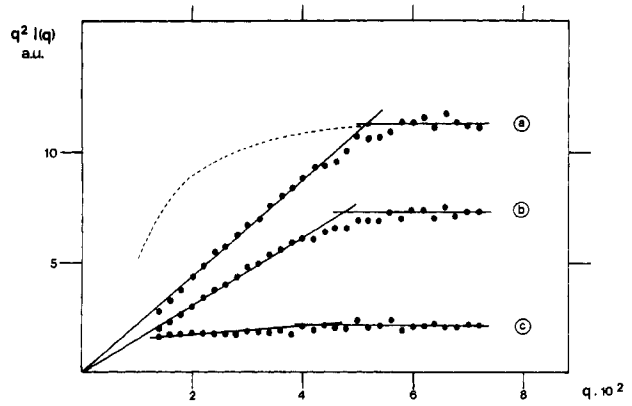

Figure 5. Kratky plot for samples B: (a) B-5.5-25; (b) B-5.5-20; (c) B-5.5-10. Dotted line is plotted according to a Gaussian form factor (relation 6) with R_g = 80 Å for case a. This shows that the first asymptotic behavior is far from that given by a Gaussian statistic.

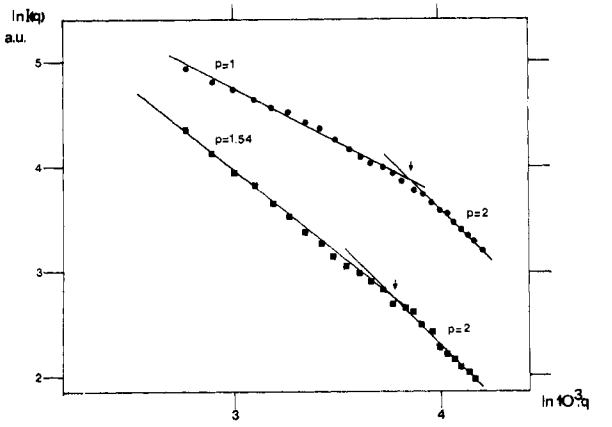

Figure 6. log $I(q)$ vs. log q for samples B: (●) B-5.5-20; (■) B-1.4-20.

havior since C_{DR} is larger or equivalent to C_D^*.

As mentioned in the first section, two hydrogenated atactic polystyrenes of different molecular weights and narrow polydispersities have been used, leading to two different situations.

High Molecular Weight APSH (M_w = 5.5 × 10⁵). Results reported in Table II and in Figures 5 and 6 show two kinds of behavior. For the highest amount of protonated atactic species (samples B-5.5-20 and B-5.5-25), the existence of an extended conformation ($I(q) \sim q^{-1}$ for $q < q^*$ possessing Gaussian subunits ($I(q) \sim q^{-2}$ for $q > q^*$) is clearly pointed out (see Figure 7b). In this case C_{DR} is close to C_D^*. For the samples containing the smallest amounts of protonated species (B-5.5-10 and B-5.5-15), the results are not so clear-cut. This arises in this case from $C_{DR} > C_D^*$ (see Figure 7a), leading to interferences in the first asymptotic domain (see Appendix). Consequently, instead of observing $I(q) \sim q^{-1}$, one notes that $I(q)$ behaves like $q^{-1.5}$. This should be compared with the results of the previous section for which one has obviously $C_{DR} \gg C_D^*$. Then the interpenetration is strong enough to smear the results as shown here.

Hereafter, it is clear that the chains are globally extended but the "collapsing" effect pointed out previously has disappeared with the addition of protonated polystyrene. This agrees with the observations on the coarseness of spherulites.[1] Indeed, if the chains were located between the crystalline lamellae instead of interfibrillar melt, one may suppose that one should observe the "collapsed" subunit structure again.

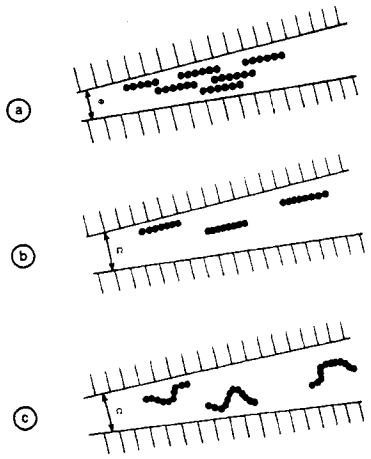

Figure 7. Schematic representation of the tagged chains within the interfibrillar melt (for samples B): (a) B-5.5-10 (C_{DR} = 11 × 10⁻² g cm⁻³); (b) B-5.5-20 (C_{DR} = 5.5 × 10⁻² g cm⁻³); (c) B-1.4-20 (C_{DR} = 5.5 × 10⁻² g cm⁻³). The points represent the Gaussian subunits.

On the other hand, the shearing probably due to the growth of the crystalline fibers is sufficient to stretch the uncrystallizable polymer. In an attempt to verify this assumption, one may compare the long relaxation time τ_m of the atactic polystyrene to the time τ_p needed for the crystalline growth front to go through the dimension of one atactic chain. Assuming that the labeled atactic chains behave like the protonated atactic surrounding, one obtains for M_w = 5.5 × 10⁵ values of R_g = 180 Å[8] and $\tau_m \simeq$ 130 s while $\tau_p \simeq$ 6–7 s[18] for X_{APS} = 20–25%. As $\tau_m > \tau_p$, one can guess that only small portions of the chain having very short relaxation times are able to recover their Gaussian behavior. From this, one may envisage a global extended conformation made of Gaussian subunits which agrees well with the SANS results.

Low Molecular Weight APSH (M_w = 1.4 × 10⁵). According to the above considerations, the use of protonated atactic polystyrene of smaller molecular weight should induce the formation of less extended conformations. For M_w = 1.4 × 10⁵, one expects the value of $\tau_m \simeq$ 4 s to be quite comparable to τ_p, which remains unchanged.

SANS experiments performed on such samples lead for $q < q^*$ to $I(q) \sim q^{-1.5}$ (Figure 6) instead of $I(q) \sim q^{-1}$ for equivalent amounts of APSH (X_{APS} = 20 and 25%). This efectively means that the chains have partially recovered their initial conformation (see Figure 7c), as was expected. Radii of gyration measurements reported in Table II support this assumption. However, for $q > q^*$ the q^{-2} dependence is found again.

It must be emphasized that the value of the exponent (p = 1.5) previously found for $C_{DR} > C_D^*$ has a different meaning than in the case where $C_{DR} \simeq C_D^*$. The former is higher than 1 due to strong interferences while the latter is due to a less extended structure.

In these samples, we then havve clearly pointed out the effect of the molecular weight of the hydrogenated atactic species on the conformation of the deuterated atactic chains. If our interpretation of the scattering curves with an extended or partially extended chain is correct, one should retrieve such results by varying both the crystallization temperature and the protonated atactic material.

Conclusion

The conformation of uncrystallizable chains within a bulk-crystallized sample has been studied through the use of small-angle neutron scattering. The experimental data clearly show the conformational modifications during the

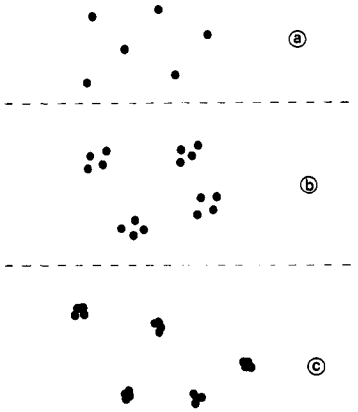

Figure 8. Schematic representation of tagged Gaussian chains (points) in a melt for different cases: (a) Gaussian chains have a uniform concentration in the melt. Then $2A_2C_DM_wP_G(q) \ll 1$, leading to $I(q) \sim P_G(q)$. (b) Gaussian chains escaped the crystallizing regions. Their concentration is no longer uniform in the sample. Then $G(r) \neq 1$ and relation 4 applies. (c) Gaussian chains interpenetrate and form clusters. Then one should use relation 18.

crystallization process. These data have been interpreted with an extended or partially extended conformation, the subunit structure of which is dependent on the concentration of hydrogenated atactic material.

Without asserting to give the exact description of the chain conformation, these interpretations are consistent with indirect observations described in the Introduction.[1-3]

In addition, it is interesting to mention that the orientation effect occurs at distances much larger than several statistical unit lengths and could not be revealed by classical techniques like evaluation of radial and tangential refractive indices of the modified spherulites.

Appendix

The rejection of deuterated atactic material out of the crystallizing regions will lead to the formation of molecular segregation into the residual amorphous material without perturbing the Gaussian statistic of the chains. Two models can be then envisaged, depending on the level of interaction between chains (see Figure 8b,c):

(i) At the beginning of the rejection, the atactic chains approach each other, first influencing the pair radial intermolecular distribution function $G(r)$ (Figure 8b). If the chains are still regarded as Gaussian, the intensity may be approximated as[21]

$$I(q) = KC_DM_w\nu^2[P(q) - 2A_2C_DM_wR(q)Q(q)] \quad (10)$$

with $R(q) = (1/N^2)[\sum_i\langle \sin qr_i\rangle/qr_i]^2$, where N is the number of links within a chain, r_i the distance between the center of mass of the chain to its any scattering unit, and $Q(q) =$

$$\int_0^\infty (1 - G(r))\frac{\sin qr}{qr}4\pi r^2\,dr \Big/ \int_0^\infty (1 - G(r))4\pi r^2\,dr$$

Using the approximation of Zimm[22] and assuming A_2 as a constant, we obtain from (10)

$$I(q) = KC_DM_w\nu^2P(q)(1 - 2A_2C_DM_wP(q)) \quad (11)$$

which can be also written

$$I(q) = KC_DM_w\nu^2P(q)/(1 + 2A_2C_DM_wP(q)) \quad (12)$$

Knowing A_2 experimentally, one can take into account the effect of $G(r)$ on the coherent scattered intensity.

(ii) If the chains have not yet been overtaken by the crystalline growth front, their "rejection concentration" increases drastically. Then, the number of contacts between labeled chains becomes very important (Figure 8c). Therefore, one must consider as a scattering model a cluster made of Gaussian chains. The existence of numerous contact points is helpful for evaluating the different vectors as drawn in Figure 9.

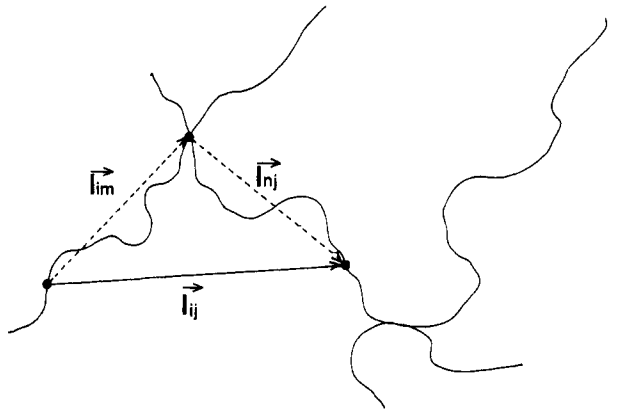

Figure 9. Schematic representation of interpenetrating labeled Gaussian chains in a cluster.

For a cluster of two chains with a total number of segments N, where $\mathbf{s}_{ij}$ is the vector joining two elements on the same chain and $\mathbf{l}_{ij}$ the vector joining two elements on different chains, we obtain

$$P_2^c(\mathbf{q}) = \left\langle \frac{1}{N^2}[2\sum_i\sum_j \exp(i\mathbf{q}\mathbf{s}_{ij}) + 2\sum_i\sum_j \exp(i\mathbf{q}\mathbf{r}_{ij})] \right\rangle \quad (13)$$

where the terms inside the brackets give the angular and thermal averages.

If π_m and π_n are the independent probabilities of finding the contact points at position m on one chain and n on the other, then

$$\pi_m = \pi_n = 2/N$$

and using $\mathbf{l}_{ij} = \mathbf{l}_{im} + \mathbf{l}_{nj}$, one obtains from (13)

$$P_2^c(\mathbf{q}) = \frac{1}{N^2}\left\langle \left[2\sum_i\sum_j \exp(i\mathbf{q}\mathbf{s}_{ij}) + \frac{8}{N^2}\sum_i\sum_j\sum_m\sum_n \exp(i\mathbf{q}(\mathbf{l}_{im} + \mathbf{l}_{nj})) \right] \right\rangle \quad (14)$$

Assuming that chains orientations are uncorrelated, one obtains finally

$$P_2^c(q) = \frac{1}{4}[2P_G(q) + 2P_G^2(q)] \quad (15)$$

where $P_G(q)$ is the form factor defined in relation 6. According to an algorithmic process, $P_{N_c}^c(q)$ for a cluster containing N_c chains can be deduced

$$P_{N_c}^c(q) = \frac{P_G(q)}{N_c^2}[(2\sum_{k=0}^{k=N_c-1}(N_c - k)P_G^k(q)) - N_c] \quad (16)$$

After the summation, relation 16 finally becomes

$$P_{N_c}^c = \frac{P_G(q)}{N_c^2}\left[\frac{2P_G^{N_c+1}(q) - N_cP_G^2(q) - 2P_G(q) + N_c}{(1 - P_G(q))^2}\right] \quad (17)$$

In this case the expression of the scattering intensity may be written

$$I(q) = C^{te}C_DN_cM_w\nu^2P_{N_c}^c(q) \quad (18)$$

From relation 18 theoretical plots exhibit characteristic

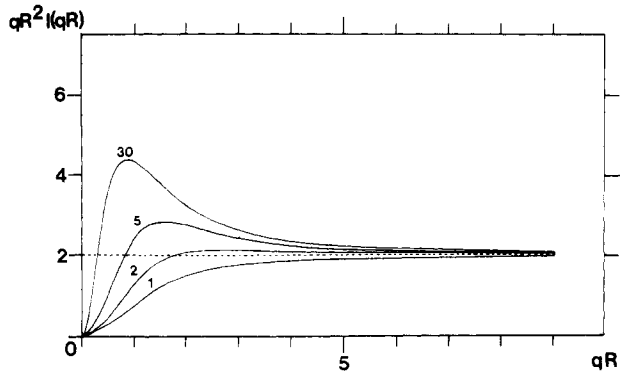

Figure 10. Theoretical Kratky plots computed from relations 17 and 18. The numbers correspond to the clustering number, N_c.

peaks in this kind of cluster using a Kratky representation (Figure 10). Such a result means that in the peak region, when $q^2I(q)$ decreases, exponents higher than $p = 2$ are found. Furthermore, this calculation may be applied to clusters made of rodlike structures by considering the form factor of rod instead of $P_G(q)$. From the above relations, it is obvious that exponents higher than $p = 1$ will be obtained, which corresponds to some results presented in this paper.

A more realistic approach would consist of taking into account a lack of inhomogeneity in the sample. Then $I(q)$ can be expressed

$$I(q) = C^{te}C_D N_{c,w} M_w \int P_{N_c}{}^c(q) f(N_c)\, dN_c$$

where $N_{c,w}$ is the weight-average number of chains in the cluster and $f(N_c)$ the distribution function of N_c. However, such an improvement of the model would not change the character of the scattering function described above.

References and Notes

(1) Keith, H. D.; Padden, F. J. *J. Appl. Phys.* **1964**, *35*, 1270.
(2) Yeh, G. S. Y.; Lambert, S. L. *J. Polym. Sci., Part A-2* **1972**, *10*, 1183.
(3) Warner, F. P.; MacKnight, W. J.; Stein, R. S. *J. Polym. Sci., Part A-2* **1977**, *15*, 2113.
(4) MacKnight, W. J.; Stoelting, J.; Karasz, F. E. *Adv. Chem. Ser.* **1971**, *No. 99*, 29.
(5) Stoelting, J.; Karasz, F. E.; MacKnight, W. J. *Polym. Eng. Sci.* **1970**, *10*, 133.
(6) Wenig, W.; Karasz, F. E.; MacKnight, W. J. *J. Appl. Phys.* **1975**, *46*, 4194.
(7) Hosemann, R.; Baghi, S. N. "Direct Analysis of Diffraction by Matter"; North-Holland Publishing Co.: Amsterdam, 1962; Chapter XVII.
(8) Cotton, J. P., et al. *Macromolecules* **1974**, *7*, 863.
(9) Kirste, R. G.; Kruse, W. A.; Schelten, J. *Makromol. Chem.* **1973**, *162*, 299.
(10) Natta, G. *J. Polym. Sci.* **1955**, *16*, 143.
(11) Guenet, J. M.; Gallot, Z.; Picot, C.; Benoit, H. *J. Appl. Polym. Sci.* **1977**, *21*, 2181.
(12) Swarcz, M. *Makromol. Chem.* **1960**, *35*, 132.
(13) Strazielle, C.; Benoit, H. *Macromolecules* **1975**, *8*, 203.
(14) Daoud, M., et al. *Macromolecules* **1975**, *8*, 804.
(15) Ibel, K. *J. Appl. Crystallogr.* **1976**, *9*, 296.
(16) Guenet, J. M.; Picot, C.; Benoit, H. *Macromolecules* **1979**, *12*, 86.
(17) Daoud, M.; de Gennes, P. G. *J. Phys. (Paris)* **1977**, *38*, 85.
(18) Keith, H. D.; Padden, F. D. *J. Appl. Phys.* **1964** *35*, 1286.
(19) Bueche, F. *J. Chem. Phys.* **1952**, *20*, 1957.
(20) Suzuki, R. Thesis, Strasbourg, 1972.
(21) Benoit, H.; Picot, C. *Pure Appl. Chem.* **1966**, *12*, 545.
(22) Zimm, B. H. *J. Chem. Phys.* **1948**, *16*, 1093.

Structural Studies of Poly(ethylenimine). 1. Structures of Two Hydrates of Poly(ethylenimine): Sesquihydrate and Dihydrate

Yozo Chatani* and Hiroyuki Tadokoro

Department of Macromolecular Science, Faculty of Science, Osaka University, Toyonaka, Osaka 560, Japan

Takeo Saegusa and Hiroharu Ikeda

Department of Synthetic Chemistry, Kyoto University, Kyoto 606, Japan.

Received August 15, 1980

ABSTRACT: X-ray structure analysis confirmed that the hygroscopic nature of crystalline linear poly(ethylenimine) is attributable to the formation of crystalline hydrates. There are two distinct hydrates in which "water of crystallization" exists stoichiometrically. One is a hydrate with a mole ratio of ethylenimine unit to water of 1/1.5, i.e., sesquihydrate. The crystals of the sesquihydrate are monoclinic with $a = 11.55$ Å, $b = 9.93$ Å, c (fiber axis) = 7.36 Å, and $\beta = 104.5°$. The space group is $C2/c$, and the unit cell contains 8 monomeric units and 12 water molecules. The other is a dihydrate; i.e., the mole ratio is 1/2. The crystals of the dihydrate are again monoclinic $C2/c$ with $a = 13.26$ Å, $b = 4.61$ Å, c (fiber axis) = 7.36 Å, and $\beta = 101.0°$. The unit cell contains 4 monomeric units and 8 water molecules. The theoretical value of water content of the crystal lattice is 38.6 wt % for the sesquihydrate and 45.6 wt % for the dihydrate. The polymer chains are planar zigzag in both hydrates, and the crystals of both hydrates consist of an alternating stack of a layer of polymer chains and a layer of water molecules arranged parallel to the *bc* plane. In particular, the water network in the dihydrate is the same as that of ordinary ice. Hydrogen bonds of the types N–H···O, O–H···O, and O–H···N play a major role in the stabilization of the crystal lattices. Irrespective of the difference in mole ratio between the two hydrates, all of the NH hydrogen atoms and H_2O hydrogen atoms in both hydrates are able to participate in hydrogen bondings, but an irregularity with respect to the disposition of these hydrogen atoms is proposed. The sesquihydrate transforms into the dihydrate on further absorption of water, retaining the uniaxial orientation, and this feature is explainable in terms of the structures of both hydrates.

Much literature in the industrial, agricultural, and biological fields has appeared for poly(ethylenimine) (PEI) and related compounds. Conventional PEI obtained from ethylenimine (EI) (PEI I) is amorphous because many branches along the polymer chain suppress crystallization.[1-5] In contrast, PEI obtained from 2-oxazoline (PEI II) is highly crystalline owing to its linear structure.[6] However, linear PEI has two characteristics which have

0024-9297/81/2214-0315$01.25/0